PHILOSOPHICAL TRANSACTIONS OF THE ROYAL SOCIETY A MATHEMATICAL, PHYSICAL & ENGINEERING SCIENCES

Experimental Studies of the Oscillatory Combustion of Hydrogen in a Stirred Flow Reactor

D. L. Baulch, J. F. Griffiths, W. Kordylewski and R. Richter

Phil. Trans. R. Soc. Lond. A 1991 **337**, 199-210
doi: 10.1098/rsta.1991.0117

Experimental studies of the oscillatory combustion of hydrogen in a stirred flow reactor

By D. L. Baulch[1], J. F. Griffiths[1], W. Kordylewski[2] and R. Richter[3]

[1] *School of Chemistry, The University of Leeds, Leeds LS2 9JT, U.K.*

[2] *Department of Heat Engineering and Fluid Mechanics, The Technical University of Wroclaw, 50-730 Wroclaw, Poland*

[3] *Department of Chemistry, University of Southampton, Southampton SO9 5NH, U.K.*

Experimental studies of the phase relations between H atoms, OH radicals and reactant temperature during the gas-phase, oscillatory combustion of hydrogen in a well-stirred flow reactor are reported. Absolute concentrations of the OH radical and the reactant temperature were measured in absorption from the vibrational–rotational structure of the laser-induced, electronically excited, OH spectrum. Relative concentrations of H atoms were obtained by multiphoton ionization, also induced by a laser. The hydrogen atoms reached their maximum concentration first during the oscillatory combustion, rising to a sharp peak followed by a rapid decay within several milliseconds. The OH radicals reached their maximum concentration about 1 ms after the H atoms. The maximum of the reactant temperature was in phase with the hydroxyl radicals. Experimental and numerical studies of the interaction that occurs between oscillations in a pair of coupled reactors are also presented.

1. Introduction

A mixture of hydrogen and oxygen at sub-atmospheric pressure in a closed reaction vessel at a temperature of *ca.* 750 K may undergo slow or even negligible reaction, or ignition may take place. The transition from slow reaction to ignition occurs at a critical vessel temperature (T_a) for a given reactant pressure (p). The ignition region lies on the high temperature side of the critical boundary in the p–T_a diagram. However, the boundary takes the mirror image of an 'S', such that there may be one or three loci of criticality with respect to increasing pressure at a given vessel temperature. In the region of multiplicity the critical conditions are termed the first, second and third ignition limits with respect to increasing pressure (Lewis & von Elbe 1987; Mulcahy 1973). Part of the second limit, associated with the present study, is exemplified in figure 4. The third limit exists at reactant pressures above 0.5 atmospheres and extends beyond one atmosphere at the lowest temperatures for its existence. In subcritical conditions the slow reaction is virtually isothermal at very low pressures (less than 50 Torr†) and hence the origins of instability are to be understood in terms of isothermal branching kinetics (Gray *et al.* 1984). Small temperature changes accompany slow reaction at higher pressures (Griffiths *et al.* 1981) and so the instability is interpreted quantitatively in terms of a chain-thermal interaction (Yang & Gray 1967; Kordylewski & Scott 1984).

† 1 Torr ≈ 133.3 Pa.

Phil. Trans. R. Soc. Lond. A (1991) **337**, 199–210
Printed in Great Britain

When hydrogen oxidation takes place in a well-stirred flow reactor, or continuous stirred tank reactor (CSTR), at low pressures, both the first and second ignition limits are observed. Their locations in the p–T_a diagram do not differ markedly from those under corresponding conditions in a closed reactor. The main distinction is that oscillatory ignition occurs in the CSTR at $p < 100$ Torr and at marginally supercritical vessel temperatures (Gray *et al.* 1984).

The oxidation occurs according to the stoichiometry

$$H_2 + \tfrac{1}{2}O_2 \rightarrow H_2O, \qquad [1]$$

from which $\Delta H^0_{298} = -242$ kJ mol^{-1}. The overall reaction is governed by a complex kinetic sequence of free-radical reactions, the chain branching (or chemical autocatalysis) features of which were identified more than 50 years ago (Semenov 1935; Hinshelwood 1942). Chinnick *et al.* (1986*a*, *b*) traced the origins of the oscillatory ignition to the kinetic autocatalysis with product inhibition coupled to the displacement of the product (water) by inflowing reactants. This signifies a relaxation oscillatory mode, which is borne out by a dependence of the oscillatory period on mean residence time, although critical slowing down also occurs by the ignition boundary (Griffiths *et al.* 1990). The principal, elementary reactions that control the existence of oscillations are as follows,

$$H + O_2 \rightarrow OH + O, \qquad \text{branching}, \qquad [2]$$

$$O + H_2 \rightarrow OH + H, \qquad \text{branching}, \qquad [3]$$

$$OH + H_2 \rightarrow H_2O + H, \qquad \text{propagation}, \qquad [4]$$

$$H + O_2 + M \rightarrow HO_2 + M, \qquad \text{propagation/termination}. \qquad [5]$$

The HO_2 radical is relatively inert and predominates in chain terminating processes at the pressures and temperatures associated with the second limit. M represents any molecular species in the system, and its intervention as a 'third body' in reaction [5] is the key to the product inhibition. In this role the water acts six times more efficiently than hydrogen and 15 times more efficiently than oxygen (Baulch *et al.* 1988*a*). Consequently, the excess water formed during ignition causes the non-autocatalytic reaction to dominate the post ignition interval until sufficient water has been displaced by the inflowing reactants to reduce the rate of reaction [5] to below that of the competitive chain branching reaction [2].

A detailed numerical analysis (Baulch *et al.* 1988*b*) gave a very satisfactory, quantitative account of the p–T_a régimes in which the oscillations existed, of the oscillatory periods and amplitudes as measured by fine-wire thermocouples, and of the reactant and molecular product concentration profiles as measured by mass spectrometry. Complex oscillatory reaction modes and birhythmicity, also found experimentally, were traced to the supplementary effects of temperature change. The calculations were based on a kinetic model comprising eight species (H_2, O_2, H_2O, H_2O_2, H, O, OH and HO_2) involved in 33 elementary reactions. The predicted evolution of concentrations and temperature during oscillatory reaction also yielded insight into the phase relations between reactive intermediates and also reactant temperature. Details of the computational methods and kinetic scheme are given elsewhere (Baulch *et al.* 1988*a*, *b*, 1990).

The present work has developed in two directions from these studies. In the first, hydrogen oxidation in the CSTR, the simplest of the gaseous, autocatalytic oscillators,

has been exploited to investigate the interaction between two oscillatory systems by setting up a diffusion couple between two stirred-flow reactors. These supplementary experimental studies and the initial results of modelling are reported in the present paper.

The second constitutes an experimental attack on the measurement of radical and atom concentrations during oscillatory combustion of hydrogen and the phase relations between the various species concentrations or their concentrations and reactant temperature. The requirement for studying phase relations is not only to have sufficiently sensitive, non-invasive methods of measurement but also to have the same temporal responses of the detection equipment when different devices are being used. Thus the methods that have been used to date, very fine thermocouples for gas temperature and probe sampling to a low-resolution mass spectrometer are ruled out because of their different and relatively slow instrumental responses (Baulch *et al.* 1988*b*). Spectroscopic methods offer viable alternatives for certain free radical species, molecular products and reactant temperature and are used in the present work.

2. Combustion apparatus and experimental procedures

Experimental features of the stirred-flow experiments have been described previously in detail (Baulch *et al.* 1988*a*, *b*, 1990). Here we summarize the main features (figure 1). Experiments were performed in an equicylindrical, Pyrex-glass, jet-stirred reactor (600 cm^3) in which a recirculating, 'toroidal' reactant flow was established about the axis of the vessel through four angled jets located in diametrically opposed pairs (Bush 1969). The reactants were pre-heated to the reactor temperature and admitted separately to the vessel.

Spectroscopic studies in the single cell were made via quartz windows, which constituted the end walls of a cylindrical reaction vessel. Each of these was mounted on the extension from a large, ground-glass cone and socket located externally to the oven. The concentric 'dead' volume surrounding these extensions was less than 200 cm^3. The exhaust duct was also fitted with an end window through which the light output associated with the ignition was detected by a photomultiplier (1P 28) to act as a trigger pulse for the spectroscopic measurements. The exhaust duct also served as an entry port for the ion probe required for the H atom studies.

Similar features for gas entry were adopted in the design of the vessel that was used to investigate the coupled oscillatory system. The main difference was that the single cell was divided at the central plane, leaving only a small aperture at the central axis that could be closed by a ground glass joint. The glass valve was controlled through a side-arm on one of the cells (figure 2). The mass transfer rate through the valve was not calibrated. The exhaust gases were drawn through a side-arm on each cell which were then coupled to a common outlet valve. Reactant temperatures were measured in each cell of the double vessel by very fine thermocouples (Pt–Pt/13 % Rh, 0.025 μm wire) protected by a thin layer of silica. Each junction was linked to a similar thermocouple located on the surface of the vessel. Even though the thermocouple response times (*ca.* 150 ms) were long compared with the timescale of the temperature change associated with ignition (less than 3 ms), the attenuated temperature records that were obtained gave very satisfactory records of oscillatory periods and the variation of amplitudes with changes of experimental conditions (Baulch *et al.* 1988*b*).

Figure 1

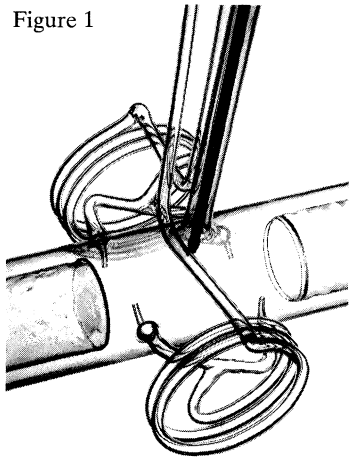

Figure 2

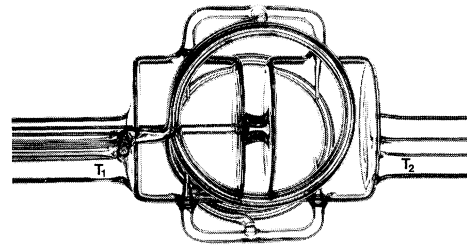

Figure 1. The single cell reaction vessel showing the preheating coils and inlets jets, the quartz windows and the electrostatic probe used for H atom detection.

Figure 2. The double cell reaction vessel showing the common preheating coils, the separate inlet jets in each cell and the ground glass link between the cells. The probe inlets for each thermocouple are also marked (T_1, T_2).

In all experiments the reaction vessel was thermostatted in a recirculating-air oven. Constant mass flow rates of hydrogen and oxygen in the chosen proportions were maintained using ASM controllers upstream, and the pressure was regulated by a needle valve downstream of the vessel. The normal procedure adopted to map out the behaviour in the p–T_a diagram was to set composition and pressure and to vary the oven temperature. By restricting the increase (or decrease) of temperature in a particular experiment to 70 K, the variation of the mean residence time was limited to less than 10%.

The spectroscopic measurements were made on the composition $2H_2+O_2$ in the vessel at a mean residence time of 1.2 s and a total reactant pressure of 16 Torr. When the vessel was maintained at 753.0 ± 0.5 K the oscillatory period for the hydrogen oxidation was 2.60 s. The period changed by less than 0.05 s over 8 h once the temperature of the system had stabilized. In some experiments the observation of more than 10^4 oscillations was necessary to construct a concentration–time profile, as described in §4.

3. Background to reactive intermediate and reactant temperature measurements

The high incident intensities, extremely high resolution and very fine line-widths of laser sources that can now be achieved have opened up the possibility of concentration and temperature measurements in combustion processes being made from the intensities of absorptions in the vibrational–rotational structure of the electronic spectra of species participating in the reaction (Cattolica 1982; Semerjian *et al.* 1982). Most applications hitherto have yielded spatial rather than temporal profiles for the OH free radical. If thermal equilibration of rotational states following translational energy transfer is assumed, the absolute populations of the individual rotational levels are proportional to the areas of the corresponding peaks in the

absorption spectrum, obtained by integration. These may then be used to determine the gas temperature and the OH radical concentration (Baulch *et al.* 1990). The relevant constants of proportionality are obtained from the transition probabilities and oscillator strengths. These data are well characterized for the $^2\Sigma$–$^2\Pi$ transition of the OH radical, having been both measured and calculated (Ankatell & Pery-Thorne 1967; Wang & Killinger 1971; Chidsey & Crosley 1980).

The multiphoton ionization method for hydrogen atom detection involves the Lyman α (^{2}S–^{2}P) transition, which is excited by three photon absorption around 364 nm. A fourth photon of the same wavelength completes the ionization process (Tjossem & Cool 1983). Ions are then detected by use of an electrostatic probe. There is, however, a competing process in which a third harmonic generation of the excited H atom occurs followed by a (1 + 1) photon ionization (Ashfold & Prince 1988). As the concentration of H atoms increases there is a proportional shift in the maximum intensity of the third harmonic generation signal to higher frequencies.

We have observed significant spectral shifts as the ion current from H^+ increases during the course of an oscillatory cycle (Baulch *et al.* 1991*a*), which is certainly associated with a change in the H atom concentration and suggests that the third harmonic generation was the predominant route to hydrogen ion formation in the present study. The overall displacement of the line maximum was also strongly affected by the spatial and temporal profile of the laser pulse and its focusing (Brewer *et al.* 1989), which cause high power densities even from a relatively low power laser. The focusing conditions also have an effect on the third harmonic generation efficiency (Bjorklund 1975). Because there was a shift in the frequency and, to some extent, in the shape of the H^+ ion spectrum in the present study (Baulch *et al.* 1991*a*) the relative concentrations of H atoms were derived from the areas of the multiphoton ionization spectra.

4. Laser absorption studies, characteristics of the spectra and data collection

(*a*) OH *radical detection and measurement*

Laser radiation in the range appropriate for the (0, 0) band absorption spectrum for electronic excitation of the OH radical (305–320 nm) was generated by an XeCl, excimer pumping laser incident upon a dye laser tunable over the range 590–630 nm. The linewidth of the dye laser was 0.17 cm^{-1} at 600 nm. The pumping laser pulse duration was 20 ns and its energy at output from the dye laser was 100–150 μJ. The output from the dye appropriate to the OH radical study (Rhodamine B, fluorescence maximum 603 nm) was frequency doubled through a KDP crystal. The beam from the dye laser was split and directed simultaneously both to a photomultiplier in order to monitor power fluctuations of the source and transmitted through the reaction vessel. The latter beam was then detected by use of an EMI 9558 QB photomultiplier, via an ultraviolet (UV) broad-band filter to attenuate extraneous signals. There was no interference from the OH emission spectrum arising from thermal excitation and chemiluminescence.

Signals from the two photomultipliers were averaged over five ignition pulses (E.G. & G. boxcar, typical gate width 20 ns). Because the maximum repetition rate for the pumping laser was 100 Hz, only one signal was recorded from each consecutive, periodic ignition. The trigger signal for the excimer laser was generated

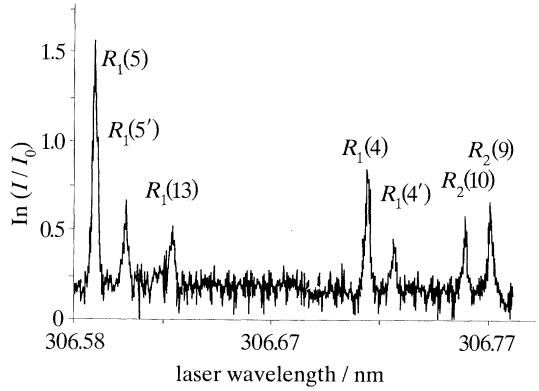

Figure 3. The vibrational–rotational fine structure in the absorption spectrum for the $^2\Sigma$–$^2\Pi$ transition of OH in the wavelength range 306.50 to 306.80 nm. The main transitions and their satellites are marked.

from the output signal of the 'slave' photomultiplier which monitored the light output from the reaction (Baulch *et al.* 1991*b*). A preset delay followed the triggering signal.

To obtain the rotational structure in the absorption spectrum for OH at a given time during the ignition, the signal was obtained at each frequency at a constant delay interval following the triggering signal (figure 3). The dye laser was advanced automatically to its next frequency (step-width, 3.5×10^{-4} nm) between the ignition pulses. The concentration–time profile of the OH radical was obtained by evaluating the spectrum of the $^2\Sigma$–$^2\Pi$ transition at different delay times.

(*b*) H *atom detection*

For H atom studies a DMQ dye pumped by the XeCl excimer laser was used to generate radiation around 364 nm (energy *ca.* 0.7 mJ/pulse, duration *ca.* 10 ns). The dye laser beam was first expanded to *ca.* 12 mm diameter and then focused into the reaction chamber by a single lens. A stainless steel, electrostatic probe (-10 V to -120 V, variable) was used to collect the positive charge produced by the laser pulse, its tip being *ca.* 2 mm from the focus of the laser beam (Cool 1984). The outer, stainless steel tube, the grounded electrode, served also as a shield from electrical noise introduced by the oven heaters and its air-recirculation fan.

Data were accumulated by repetitive laser firing at constant delay time on five successive ignitions at each incident wavelength, as previously. Variations of hydrogen atom concentration throughout ignition were reconstructed from the area under the ionization signal obtained over a range of wavelengths, after different delay intervals from the trigger signal. The complete MPI spectrum and the distribution of arrival times of ions at the collector are reported elsewhere (Baulch *et al.* 1991*b*).

5. Experimental results

(*a*) p–T_a *regions of oscillatory ignition and the response to coupling of two jet-stirred flow reactors*

Oscillatory ignition was confined to a relatively small region adjacent to the second ignition limit in the p–T_a ignition diagram. The conditions for the mixture $2H_2 + O_2$ in a 600 cm^3 cylindrical vessel are shown in figure 4. The location of the second limit

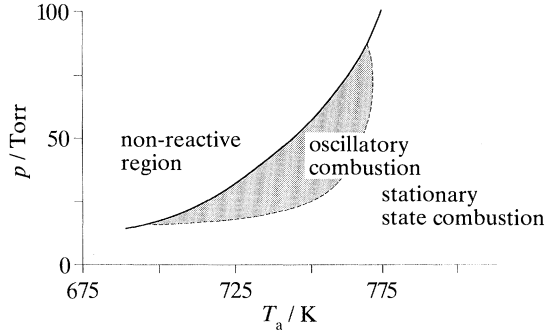

Figure 4. p–T_a régimes for the existence of stationary-state reaction and oscillatory ignition for the composition $2H_2+O_2$ in a jet-stirred, cylindrical reactor (500 cm^3) at a mean residence time of 1.2 s.

varies with reactant composition, but not very greatly (Baulch *et al.* 1988*a*). Nor is the dependence on vessel size very strong (Griffiths *et al.* 1981). Thus the location of the second ignition limit in each cell of the double vessel was not very different from that illustrated in figure 4 for the larger, single cell reactor. By contrast, the oscillatory period and also the high-temperature limit at which oscillatory ignition gave way to a stable stationary-state reaction was strongly dependent on the mean residence time and on reactant composition.

The attainment of the same compositions and flow rates in each cell of the double reactor, when a common source of the hydrogen and oxygen was used, was conditional upon the inlet jets being of identical size in each cell. Even small differences in jet size and cell volume, arising during manufacture of the vessel, gave slightly different flow rates (and hence mean residence times) and slightly different mixtures within each cell of the double vessel. The geometric differences between the cells were exploited in the results described below.

The temperature change associated with reaction in each cell of the double vessel when there was no direct coupling through the diffusion leak is shown in figure 5*a*. Conditions were chosen such that a high temperature stationary state was maintained in cell 1 while oscillations of long period ($\tau = 6.66$ s, frequency $\nu = 0.15$ Hz) occurred in cell 2, the reactant pressures and cell wall temperatures being the same. There was some interaction between the two, manifest as a small, damped oscillatory disturbance of the stationary-state reaction, which probably occurred via the link in the exhaust port upstream of the pressure-controlling needle valve. The oscillatory nature of the induced disturbances identifies the character of the stationary state as that of a stable focus (Griffiths & Scott 1988).

When the diffusion couple was fully opened, without change of reactant pressure, flow rate or vessel temperature, there was a complete entrainment, such that oscillatory reaction then occurred at the same frequency and amplitude in each cell (figure 5*b*). The period was almost $\frac{1}{4}$ of that which was observed in the uncoupled cell 2 (i.e. frequency = 3.6ν). More complex interactions were observed to accompany a partial restriction of the aperture. The rate of transport through the diffusion couple was not measured.

(*b*) OH *radical*, H *atom and reactant temperature measurements in a single reactor*

The graphs taken from the absorption spectrum of OH obtained yield a standard deviation of 250 K (Baulch *et al.* 1990). Consequently the OH radical concentrations derived from their intercepts have an error of $\pm 30\,\%$. However, the observed time

PHILOSOPHICAL TRANSACTIONS OF THE ROYAL SOCIETY A MATHEMATICAL, PHYSICAL & ENGINEERING SCIENCES

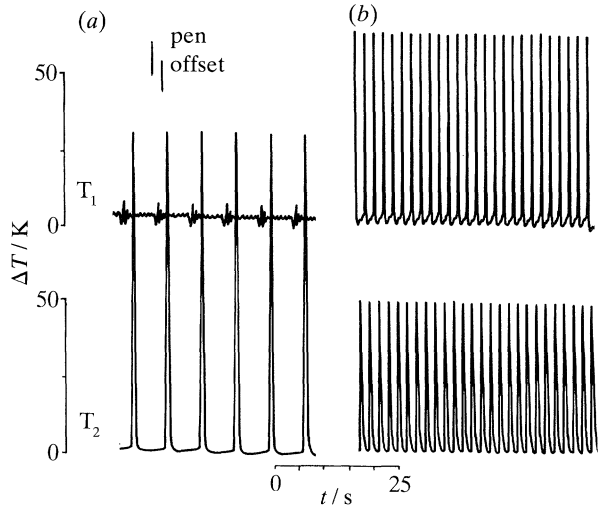

Figure 5. Temperature–time records measured simultaneously in each cell of the double vessel during reaction of H_2+O_2 at $p = 15$ Torr, $t_{res} = 4$ s and $T_a = 749$ K. (*a*) Uncoupled reaction, (*b*) fully coupled reaction.

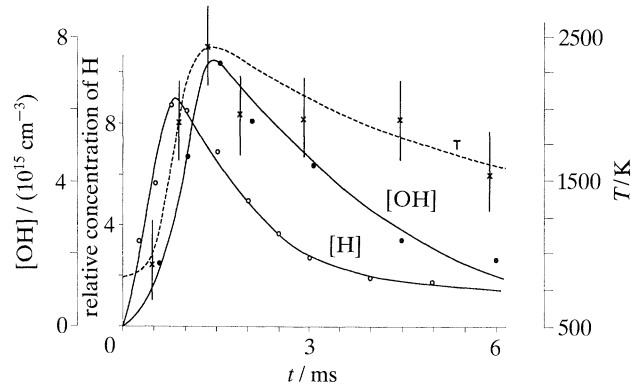

Figure 6. Temperature–time and OH radical concentration–time profiles measured from the vibrational–rotational spectrum of the OH radical, and the relative H atom concentration–time profile obtained from multiphoton ionization studies.

dependences were sufficiently accurate to show that the measured temperature profile followed very closely the rise in OH concentration in each system (figure 6). The temperature decay was several orders of magnitude slower than that of the OH concentration because it was controlled by the heat transfer rate to the vessel walls (Baulch *et al.* 1990). The interval over which the gas temperature could be interpreted was restricted to the period during which distinct OH radical signals could be detected. This was approximately 10 ms. A maximum of about 2500 ± 250 K was measured during oscillatory ignition, which may be expected since the rate of reaction was sufficiently fast for the temperature change to be virtually adiabatic.

The integrated areas of the MPI signals, which represent relative H atom concentrations, are also plotted as a function of time in figure 6. There is a very rapid rise to a sharp maximum at *ca.* 1 ms after the trigger signal. Not only is the maximum concentration of the H atom reached nearly 1 ms before that of the OH

radical, but also its measured concentration has decayed by 25% by the time the maximum of the OH concentration is attained.

7. Discussion

Hydrogen combustion constitutes the simplest of the gas-phase oxidations, involving the four molecular species, H_2, O_2, H_2O and H_2O_2, and the four free-radicals or atoms H, O, OH, and HO_2. This is, therefore, a nine-variable system when temperature change is included, and nonlinearities arise in it both from the temperature dependence of the elementary reactions and from quadratic autocatalysis (Baulch *et al.* 1988*a*, *b*). Detailed kinetic models of the chemistry may have considerable numbers of reactions (Dixon-Lewis 1975, 1983; Westbrook & Dryer 1984, Maas *et al.* 1986). Our own simulations of hydrogen oxidation incorporate 33 elementary reactions (Baulch *et al.* 1988*a*, *b*).

(*a*) *Modelling of the coupled oscillatory system*

The detailed thermokinetic model used previously (Baulch *et al.* 1988*a*, *b*) was adapted to interpret the interaction in the double cell vessel. The rate of mass transport was set up in its simplest form, characterized by a mass transfer coefficient at a concentration step for each species between each cell. Here we focus on the effect of transport of H atoms alone. In practice, the mass transport was complicated by pressure fluctuations during the course of oscillations. There was negligible heat transfer between the two cells.

To establish different numerical behaviour in each cell for the same initial reactant pressures and flows at the same wall temperature, different surface termination rate constants were assigned for the H atoms (10 s^{-1} in cell 1 and 250 s^{-1} in cell 2). These gave the predicted concentration–time profiles shown in figure 7*a*, which represented a high temperature, fully reacted state in cell 1, and oscillatory ignition of period 3.8 s in cell 2 under the same conditions. Fully entrained oscillatory ignitions occurred in each cell at a period of 2.2 s when the mass transport term of H atoms between the cells was set at 20 s^{-1} (figure 7*b*). The dominant role of H atoms is to be expected in view of their contribution to chain branching via reaction [2], and enhanced by their extremely high diffusion rates, in practice.

(*b*) *Comparisons between the experimental* H *atom*, OH *radical and reactant temperature profiles and their numerical simulation*

The onset of ignition in the numerical analysis was related to that of the spectroscopic study by matching the numerically predicted maximum of the OH concentration to the time at which the experimental maximum was observed. The calculated maximum concentration OH was approximately twice that measured experimentally (figure 8). The predicted reactant temperature reached its peak (2700 K) in phase with the rising OH radical concentration but it then remained virtually unchanged throughout the interval corresponding to that for its experimental measurement (10 ms). This is attributable to the much slower thermal relaxation than the rate of free radical decay. The behaviour agrees closely with that observed experimentally. The predicted onset of a subsequent ignition followed some 3 s later at the simulated conditions for the radical and atom concentration measurements.

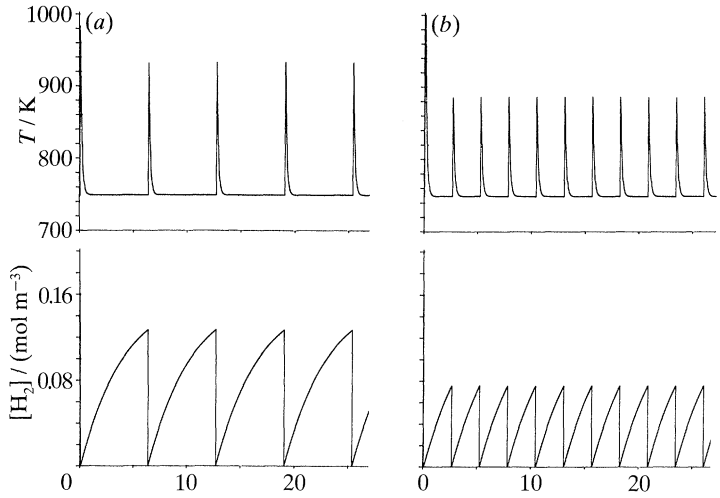

Figure 7. Simulated concentration–time profiles for hydrogen and thermocouple records in cell 2 of the double vessel under conditions as specified in figure 5. (*a*) Uncoupled reaction, (*b*) fully coupled reaction.

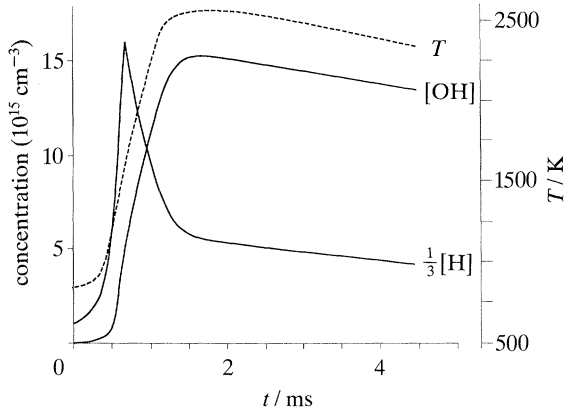

Figure 8. Simulated H atom OH radical and temperature–time profiles during the oscillatory combustion of hydrogen. The conditions are the same as those for figure 6.

The predicted maximum in the concentration profile for the H atom preceded the maximum in OH concentration (less than 1 ms) and was in very good agreement with the relative concentration profile for H which was obtained experimentally (figure 8). The H atoms were predicted to reach a maximum concentration of 4.5×10^{-16} cm^{-3}. It is difficult to generate known amounts of hydrogen atoms for the purposes of calibration of the multiphoton ionization measurements at the concentrations predicted here. Moreover, we do not have direct evidence that there is a linear relation between signal strength and atom concentration at the levels present in this particular system. However, the agreement between the measured and calculated OH concentration and temperature profiles, and of other features of the oscillatory reaction, is sufficiently good (Baulch *et al.* 1988*b*) that numerical modelling of this kind may prove to be a viable way for calibration of the MPI technique in applications to other systems.

Since the oscillatory temperature change reaches its maximum simultaneously with the OH radical concentration, the phase differences that exist between the

independent variables during oscillatory reaction must relate to the principal chain propagating species and their kinetic interactions, and is identified in the present work as a phase difference between H atoms and OH radicals. There may yet be other phase differences associated with the HO_2 radical, as indicated by numerical modelling (Baulch *et al.* 1988*b*).

The authors thank SERC, the Royal Society and British Gas for financial support. We are also pleased to acknowledge the outstanding skill of C. J. Gascoigne and M. Holmes in the construction of reaction vessels and other equipment.

References

Anketell, J. & Pery-Thorne, A. 1967 *Proc. R. Soc. Lond.* A **301**, 343–350.

Ashfold, M. N. R. & Prince, J. D. 1988 *Contemp. Phys.* **29**, 125–157.

Baulch, D. L., Griffiths, J. F., Pappin, A. J. & Sykes, A. F. 1988*a* *J. chem. Soc. Faraday Trans. I* **84**, 1575–1586.

Baulch, D. L., Griffiths, J. F., Pappin, A. J. & Sykes, A. F. 1988*b* *Combust. Flame* **73**, 163–185.

Baulch, D. L., Griffiths, J. F., Johnson, B. & Richter, R. 1990 *Proc. R. Soc. Lond.* A **430**, 151–166.

Baulch, D. L., Griffiths, J. F. & Richter, R. 1991*a* *Proc. R. Soc. Lond.* A **434**, 399–412.

Baulch, D. L., Griffiths, J. F. & Richter, R. 1991*b* *Combust. Flame* **85**, 271–274

Brewer, L. R., Buchinger, F., Ligare, M. & Kelleher, D. E. 1989 *Phys. Rev.* A **39**, 3912–3923.

Bush, S. F. 1969 *Trans. Instn chem. Engrs* **74**, T59–T72.

Bjorklund, G. C. 1975 *IEEE J. Quantum Electron.* **11**, 287–296.

Cattolica, R. J. 1982 *Combust. Flame* **44**, 43–60.

Chidsey, I. L. & Crosley, D. R. 1980 *J. quant. Spectrosc. radiat. Transfer* **23**, 187–199.

Chinnick, K. J., Gibson, C., Griffiths, J. F. & Kordylewski, W. 1986*a* *Proc. R. Soc. Lond.* A **405**, 117–128.

Chinnick, K. J., Gibson, C. & Griffiths, J. F. 1986*b* *Proc. R. Soc. Lond.* A **405**, 129–142.

Cool, T. A. 1984 *Appl. Optics* **23**, 1559–1572.

Dixon-Lewis, G. 1975 *Phil. Trans. R. Soc. Lond.* A **292**, 45–90.

Dixon-Lewis, G. 1983 *Combust. Sci. Tech.* **34**, 1–30.

Gray, B. F. & Yang, C. H. 1967 In *Proc. 11th Symp.* (*Int.*) *on Combustion*, pp. 1057–1061. Pittsburgh, Pennsylvania: The Combustion Institute.

Gray, P., Griffiths, J. F. & Scott, S. K. 1984 *Proc. R. Soc. Lond.* A **394**, 245–258.

Griffiths, J. F., Scott, S. K. & Vandamme, R. 1981 *J. chem. Soc. Faraday Trans. I* **77**, 2265–2270.

Griffiths, J. F. & Scott, S. K. 1988 *Prog. Energy Combust. Sci.* **13**, 161–197.

Griffiths, J. F., Kordylewski, W., Pappin, A. J. & Sykes, A. F. 1990 *Spatial inhomogeneities and transient behaviour in chemical kinetics* (ed. P. Gray, G. Nicolis, F. Baras, P. Borckmans & S. K. Scott), pp. 237–253. Manchester University Press.

Hinshelwood, C. N. 1942 *The kinetics of chemical change*. Oxford University Press.

Kordylewski, W. & Scott, S. K. 1984 *Combust. Flame* **57**, 127–139.

Lewis, B. & von Elbe, G. 1987 *Combustion, flames and explosions in gases*, 3rd edn. New York: Academic Press.

Maas, U., Raffel, B., Wolfrum, J. & Warnatz, J. 1986 In *Proc. 21st Symp.* (*Int.*) *on Combustion*, pp. 1869–1876. Pittsburgh, Pennsylvania: The Combustion Institute.

Moore, C. E. 1949 *Atomic energy levels*, vol. 1. NBS circular.

Mulcahy, M. F. R. 1973 *Gas kinetics*. London: Nelson.

Semenov, N. N. 1935 *Chemical kinetics and chain reactions*, 4th edn. Oxford University Press.

Semerjian, H. G., Santoro, R. J., Emmerman, P. J. & Goulard, R. 1982 *Temperature; its measurement and control in science and industry* (ed. J. F. Schooley), vol. 5, pp. 649–669. American Institute of Physics.

Tjossem, P. J. H. & Cool, T. A. 1983 *Chem. Phys. Lett.* **100**, 479–483.

Wang, C. C. & Killinger, D. K. 1971 *Phys. Rev. Lett.* **39**, 929–932.

Warnatz, J. 1985 In *Combustion chemistry* (ed. W. C. Gardiner), p. 197. New York: Springer.

Westbrook, C. K. & Dryer, F. L. 1984 *Prog. Energy Combust. Sci.* **10**, 1–47.

Yang, C. H. & Gray, B. F. 1967 In *Proc. 11th Symp.* (*Int.*) *on Combustion*, pp. 1099–1106. Pittsburgh, Pennsylvania: The Combustion Institute.

PHILOSOPHICAL TRANSACTIONS OF THE ROYAL SOCIETY A MATHEMATICAL, PHYSICAL & ENGINEERING SCIENCES

Figure 1

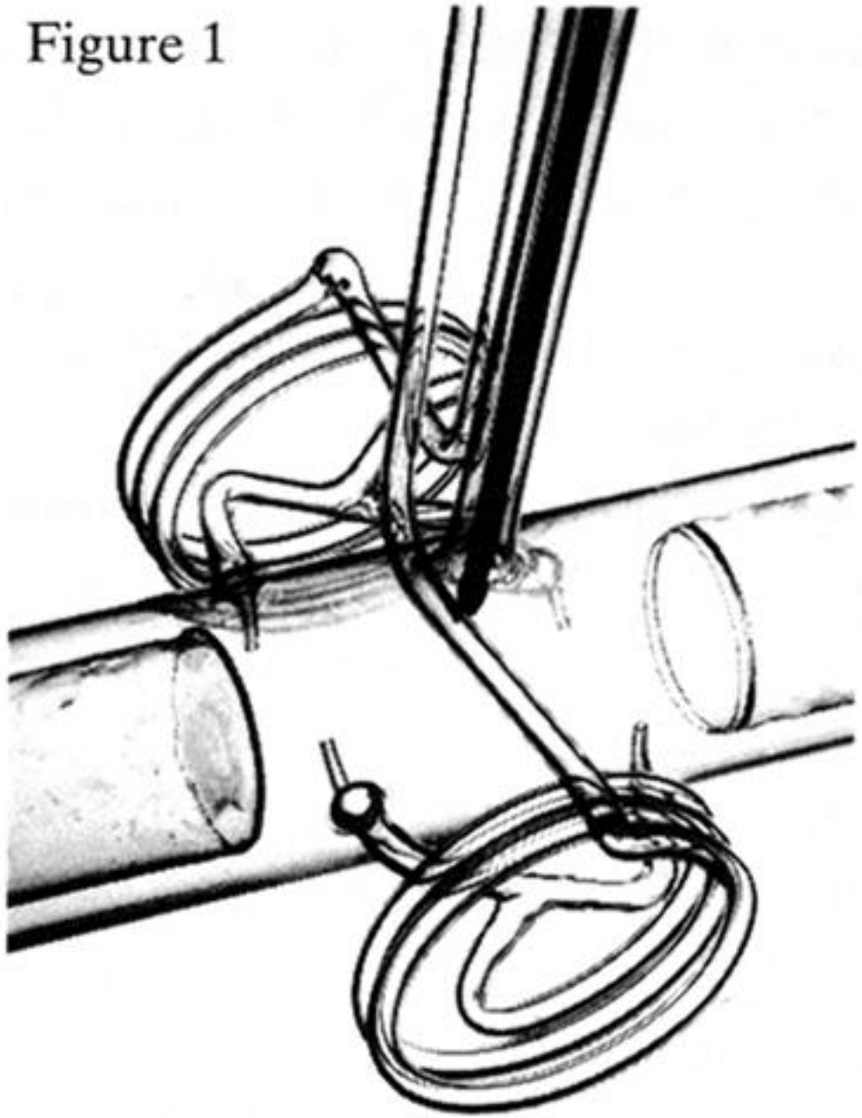

Figure 2

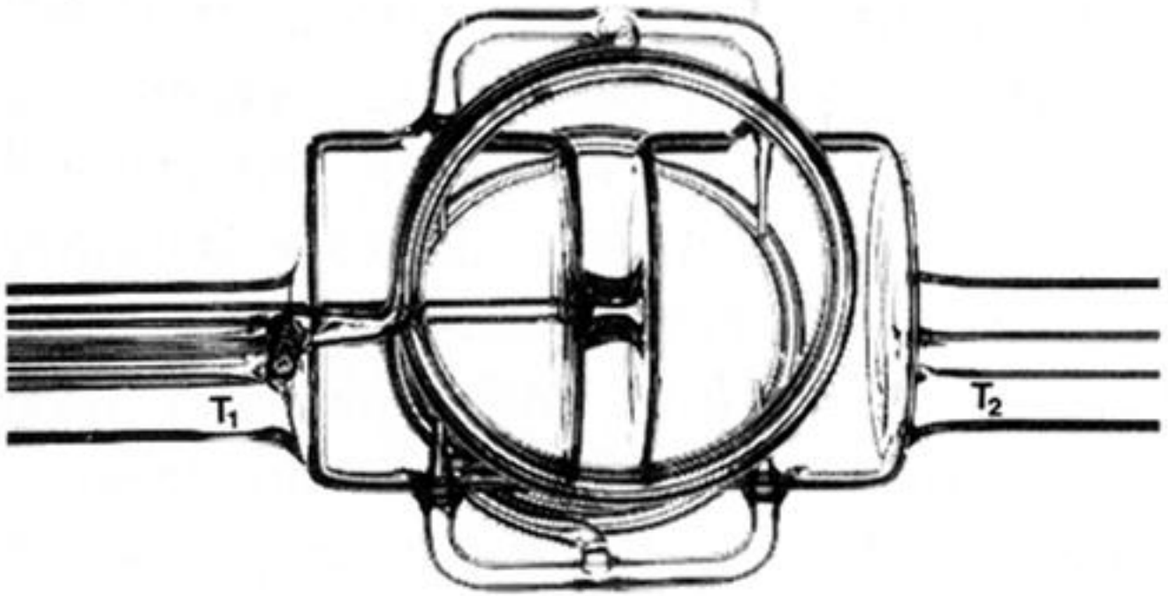

igure 1. The single cell reaction vessel showing the preheating coils and inlets jets, the quartz indows and the electrostatic probe used for H atom detection.

igure 2. The double cell reaction vessel showing the common preheating coils, the separate inlet ts in each cell and the ground glass link between the cells. The probe inlets for each thermocouple re also marked (T_1, T_2).